OBSERVATION OF HELIUM TWO-PHASE FLOWS IN A PIPE

Mamoru Oike[1], Takashi Tokumasu[1], Kenjiro Kamijo[1]
[1]Institute of Fluid Science, Tohoku University
Sendai, Miyagi, 980-8577, JAPAN

Abstract

Applications using cryogenic fluid generally encounter obstacles or complex pipe shapes such as an orifice or a converging-diverging nozzle. Therefore, a flow visualization study on two-phase cryogenic flow passing through a convergent-divergent nozzle or an orifice nozzle installed in a horizontal pipe is carried out to clarify the fundamental characteristics of the transient growth process of helium cloud cavitation. The pipe is filled with pressurized cryogenic liquid and flow immediately occurs when the on-off valve is opened. The transient growth process of the cloud cavitation induced by flow through the throat is observed from high-speed video images. Comparisons between the high-speed observations and the pressure measurements indicates that the transient growth process can be divided into two different steps by taking into account the transition point based on the observational results. Furthermore, it is confirmed that there are two types of the pressure instability in blowdown tests: one is the instability induced by density wave oscillation and the other is that induced by acoustic wave oscillation.

1 Introduction

Cryogenic flow systems that include two-phase flow are widely used in LNG (liquefied Natural Gas) plants, aerospace technology, superconductivity technology, and many other engineering applications. Thus, the investigation of the two-phase flow characteristics of cryogenic fluids such as liquid helium is very interesting and important not only in the basic study of the hydrodynamics of cryogenic fluid but also for providing solutions to problems related to practical engineering applications of cryogenic two-phase flow (Filina and Weisend 1996). Cryogenic fluids are characterized by large compressibility as compared with fluids, such as water, at room temperature, by a small difference in density between vapor and liquid phases and by a small latent heat of vaporization. These unique characteristics of cryogenic fluids can be utilized to realize high performance in fluid apparatuses, such as the two-phase operation of inducers for liquid rocket turbopumps (Cheremisinoff 1989, Kamijo et al. 1993, King 1972). Cryogenic flow has been investigated for many years; however, only little information useful for clarifying the fundamental characteristics of the transient growth process of helium cloud cavitation has been obtained by theoretical and experimental studies (Filippov 1999, Huang and Van Sciver 1994, Sauvage-Boutar et al. 1987). One of the main reasons for the difficulty in the study of liquid He is that experimental results are insufficient for the validation of mathematical models because of the difficulty nature of techniques for visualizing helium two-phase transient flow.

In the present study, a flow visualization of two-phase cryogenic flow passing through a convergent-divergent nozzle or an orifice nozzle installed in a horizontal pipe was carried out to clarify the fundamental characteristics of the nucleation and transient growth process of helium cloud cavitation based on a comparison between liquid helium (He) and liquid nitrogen (N_2). Furthermore, flow instability is herein discussed based on instable pressure oscillations measured in blowdown tests.

2 Experiment

Figure 1 shows a schematic of the simple blowdown apparatus employed. The test apparatus consists of a cryogenic supply tank, a flow visualization section installed in a horizontal pipe with vacuum insulation, a remote controlled on-off valve, a by-pass with a needle valve, and a buffer tank. The blowdown tests were carried out using two types of the throat configuration installed in the visualization section, shown in Fig. 2. One is a convergent-divergent nozzle (C-D nozzle) with a throat diameter of 2 mm and a contraction area ratio of 1/25. The other is a 15-mm-long rectangular orifice nozzle with a throat cross section 2 mm by 8 mm, having a contraction area ratio of 1/5. The C-D nozzle and both sides of the orifice are made of the quartz glass to permit observation of the two-phase flow phenomenon induced by flow through the throat. A 2.1-m-long pipe connects the supply tank and the throat. The length of the pipe between the throat and the on-off valve is 3.0 m. A 3.5-m-long line from the supply tank with the above-mentioned visualization section is installed in a vacuum chamber.

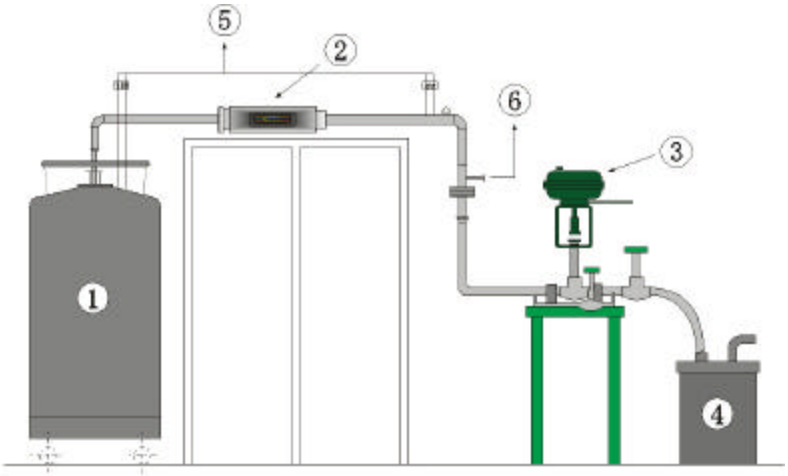

①Liquid tank, ②Visualization section,
③Remote control valve, ④Buffer tank,
⑤Computer,⑥Vacuum pump

Fig. 1 Cryogenic blowdown apparatus

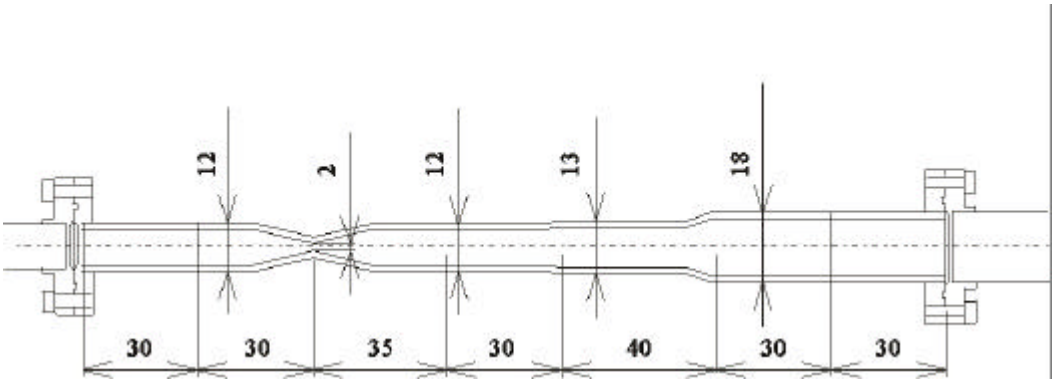

(a) Convergent-divergent nozzle (C-D nozzle) of circular cross section

Flow direction →

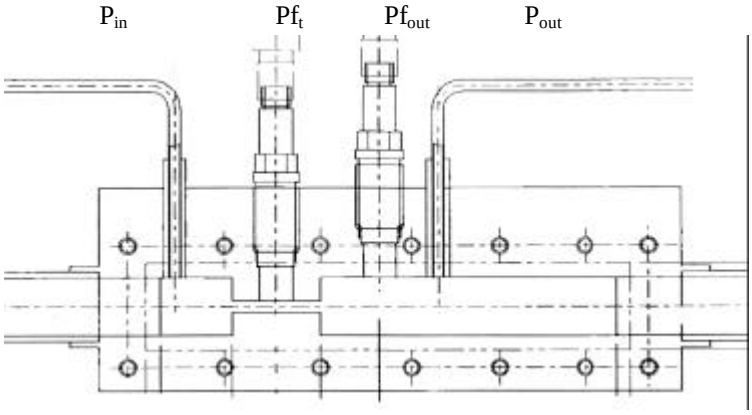

(b) Orifice nozzle with rectangular cross section of 2 mm x 8 mm and 15 mm long
(Cross section of upstream and downstream parts: 10 mm x 8 mm rectangle)

Fig. 2 Schematic of flow visualization section

The line was filled with pressurized cryogenic liquid and flow immediately occurred when the on-off valve was opened. Since the cryogenic liquid was continuously supplied from the storage tank, the flow was accelerated at the nozzle throat in the visualization section. Thus, boiling occurred within the throat due to a drop in pressure. The nucleation and transient growth process of the cloud cavitation were observed by a high-speed video camera, maximum frame speed of which is 40,500 pps. Pressures were measured by strain-gauge-type pressure sensors and the temperature was measured by a resistance thermometer at the following positions: T_0, P_0: temperature and pressure in the supply tank; P_1: pressure 1.5 m downstream of the nozzle throat; P_3: pressure 3.0 m downstream of the nozzle throat; P_{in}: pressure 0.01 m upstream of the orifice inlet; P_{out}: pressure 0.02 m downstream of the orifice outlet; Pf_t: pressure fluctuation in the middle of the orifice throat; Pf_{out}: pressure fluctuation 0.01 m downstream of the orifice outlet. The blowdown test conditions are summarized in Table 1. The buffer tank opens into atmospheric pressure.

Table 1 Test conditions

Fluid	Throat	P_0 (MPa)	T_0 (K)	$P_{0,s}$ (MPa)	P_c (MPa)
N_2	Orifice nozzle	0.239 – 0.251	77.1 – 77.4	0.0994 – 0.1021	3.40
N_2	C-D nozzle	0.263 – 0.284	77.1 – 77.2	0.0994 – 0.0996	3.40
He	C-D nozzle	0.289 – 0.291	4.5	0.1299	0.2275

$P_{0,s}$: Saturation pressure at T_0, P_c : Critical pressure

3 Observation of transient two-phase flow

Figure 3 shows pressure measurements obtained in a blowdown test with N_2 flowing through the orifice nozzle. Since the needle valve installed in the by-pass was opened slightly to maintain liquid phase flow in the visualization section before the opening of the on-off valve in the main line, there were small oscillations of P_{in} and P_{out} with the same frequency of about 15.5 Hz. The main flow immediately occurred when the on-off valve was opened. Therefore, the downstream pressures, P_{out} and P_1, quickly decreased with instable oscillations, and P_{in} slightly decreased with a large damping oscillation. High-speed observations of N_2 flowing through the orifice nozzle are shown in Fig. 4. Each video image was obtained at the point marked in Fig. 3 by the same letter as the caption index. Figures 4 (a) and 4 (b) show that the initial nucleation of the cloud cavitations occurred at the inlet edges of the throat, which indicates that a decreasing pressure gradient created separation bubbles of reverse flow just inside the throat. Each cloud cavitation grew downstream and the cavitations combined with each other at 5 mm downstream of the inlet in Fig. 4 (c). As shown in Fig. 3, the value of P_{out} rapidly decreased from (b) to (d), so that the cloud cavitation flowed from the throat outlet in Fig, 4 (d). Comparison between Fig. 3 and Fig. 4 indicates that the extent of the cloud cavitation in the downstream zone depended on the value of P_{out} after the cloud cavitation had flowed out of the throat. Therefore, the extent of the cloud cavitation oscillated with the vibration of P_{out} value, as shown in Figs. 4 (e) – (k). Finally, the cloud cavitation grew over the whole downstream zone in the visualization section at the time of t = 1.767 s, i.e., t_0 = 1.170 s from the opening of the on-off valve, in Fig. 4 (l).

The pressure fluctuations, Pf_t and Pf_{out}, in the middle of the throat and in the downstream part were measured by piezoelectric pressure sensors with a discharge time constant of 2.0 s. As shown in Fig. 5, Pf_t and Pf_{out} showed nearly synchronous fluctuations up to 1.19 s, and after that the correlation of Pf_t with Pf_{out} disappeared. In Fig. 3, the influence of P_{out} on P_{in} also disappeared at the same time. Therefore, it can be considered that the two-phase flow is choked within the throat after t = 1.19 s and that the critical pressure ratio is 0.60. The value of Pf_t rapidly decreased from (c) to (d) and reached its minimum value. After that, the value of Pf_t increased monotonically due to the exponential decay of the charge signal, which means that the average pressure in the throat maintained nearly a constant value after (d), except for around (e). However, after having minimum value, Pf_t showed a specific fluctuation, which was characterized by a relatively large amplitude and a higher frequency. Based on comparison with the observations, it can be considered that these features of the pressure fluctuation are induced by the full development of two-phase flow within the orifice throat. Therefore, it is confirmed that we can identify the fully developed cloud cavitation within the orifice throat by measuring the pressure fluctuation.

In the case of blowdown tests of flow through the convergent-divergent nozzle (C-D nozzle), P_0, P_1 and P_3 were mainly measured. Figure 6 shows pressure measurements of a blowdown test of N_2 flowing through the C-D nozzle. The main flow occurred when the on-off valve was opened, so that P_1 and P_3 quickly decreased with damping oscillations. Both of the damping oscillations were nearly synchronous. Figure 7 shows high-speed observations obtained at the points in Fig. 6 indicated by the same letters as the caption indexes. Since the two-phase flow was observed as a shadowgraph, the cloud cavitation can be seen as a dark shadow. As shown in Figs. 7 (a) – (d), the initial nucleation of the cloud cavitation was observed at t_0 = 0.886 s from the opening of the on-off valve. Figures 7 (e) – (j) present a typical nucleation-collapse cycle of the cloud cavitation with a period of about 1 ms.

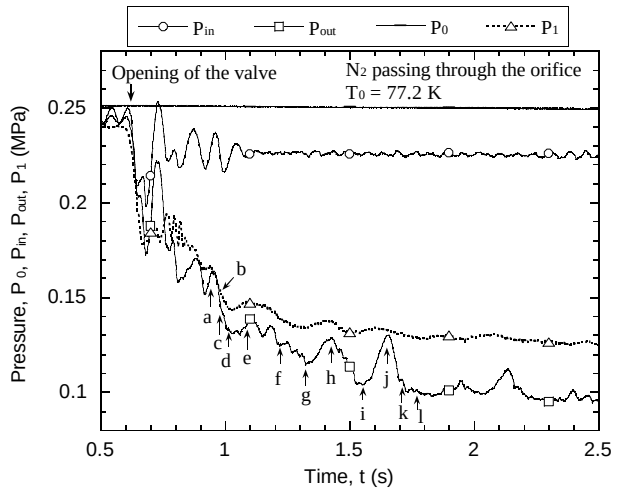

Fig. 3 Pressure measurements of N_2 flow, orifice nozzle

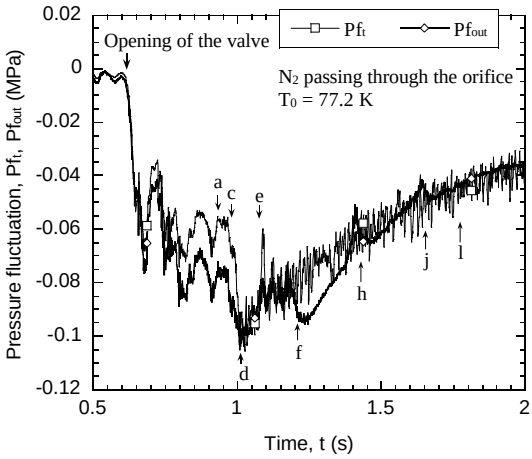

Fig. 5 Pressure fluctuation of N_2 flow, orifice nozzle

Orifice → Downstream

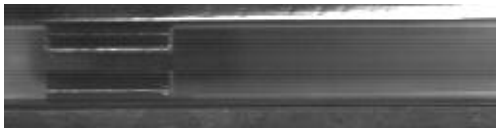

(a) t = 0.941 s (0.344 s ; from opening of the valve)

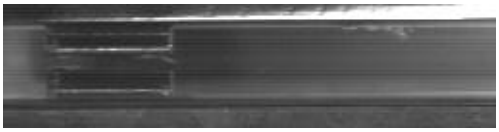

(b) t = 0.974 s (0.377 s)

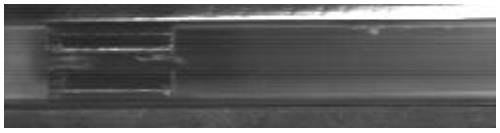

(c) t = 0.978 s (0.381 s)

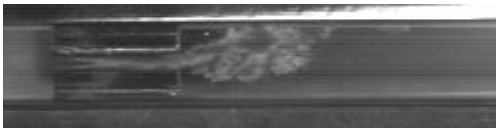

(d) t = 1.009 s (0.412 s)

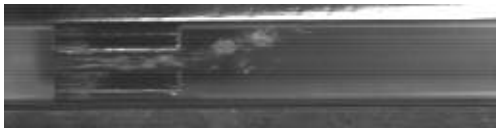

(e) t = 1.084 s (0.487 s)

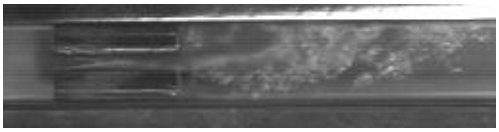

(f) t = 1.208 s (0.611 s)

(g) t = 1.323 s (0.726 s)

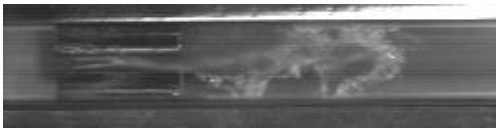

(h) t = 1.427 s (0.830 s)

(i) t = 1.553 s (0.956 s)

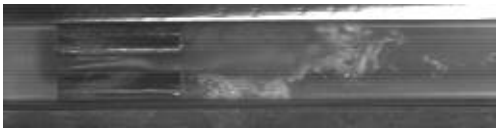

(j) t = 1.656 s (1.059 s)

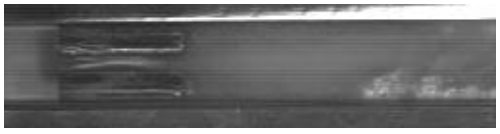

(k) t = 1.717 s (1.120 s)

(l) t = 1.767 s (1.170 s)

Fig. 4 High-speed observations of N_2 flowing through the orifice nozzle

The period increased with time and reached about 2 ms near point (k). The cloud cavitation was not always observed in the throat downstream section during (a) to (k). At intervals, the cloud cavitation disappeared from the visualization section. In Fig. 7 (k), the upstream interface between the cloud cavitation and the liquid phase was fixed at the nozzle throat, and after that cloud cavitaion was always observed. The extent of the cloud cavitation gradually increased downstream with some fluctuation. Finally, the cloud cavitation grew over the whole downstream zone in the visualization section at the time of t_0 = 1.670 s in Fig. 7 (l).

Pressure measurements during a blowdown test of He flowing through the C-D nozzle are presented in Fig. 8. After opening of the on-off valve, P_1 and P_3 rapidly decreased with small damping oscillations. Comparison with the N_2 tests clearly shows that the reduction rate of pressure is much higher than that of N_2, so that the amplitude of the damping oscillation is much smaller than that of N_2. Figure 9 shows high-speed observations obtained at the points marked in Fig. 8 by the same letters as the caption indexes. Figures 9 (a) – (d) show that the initial nucleation of the cloud cavitation was observed at t_0 = 0.065 s from the opening of the on-off valve. In contrast with N_2, the He cloud cavitaion was continuously produced near the nozzle throat and never disappeared from the visualization section after the initial nucleation. As shown in Figs. 9 (e) – (j), the extent of the cloud cavitation inceased downstream with time and grew over the whole downstream part in the visualization section at the time of t_0 = 0.642 s. In Fig. 7, the N_2 cloud cavitation can be seen as a dark shadow; however, the cloud cavitation of He is observed as a dim shadow in Fig. 9, which indicates that the He cloud cavitation consists of smaller bubbles than those of N_2. Therefore, the liquid-vapor mixture in the He cloud cavitation can be regarded as being more homogeneous than that of N_2.

Assuming that the nucleation of the cloud cavitation occurs at the saturartion pressure, $P_{0,s}$, of the T_0 value, i.e., isothermal flow in the throat upstream line, the pressure recovery ratio, R_p, at the downstream position in which P_1 is measured is given by $R_p = (P_1 - P_{0,s})/(P_0 - P_{0,s})$. Figure 10 shows the relationships between the pressure recovery ratio and time from the opening of the on-off valve obtained in the blowdown tests of He and N_2 under cavitating conditions. The first plot of each test shows the value of R_p obtained at the initial nucleation of the cloud cavitation and the last plot shows that obtained when the cloud cavitation had grown over the whole downstream zone in the video image. The value of R_p at the He initial boiling is at least more than 0.6 and is much higher than that of N_2. However, the R_p value of the last plot in the He test shows nearly the same value as that of the N_2 test flowing through the C-D nozzle. Figure 10 shows that R_p of each He test decreases rapidly and monotonically with time; however, R_p of each N_2 test has a transition point. In the test of N_2 flowing through the C-D nozzle, the transition point corresponds to point (k) in Fig. 7, at which the upstream interface of the cloud cavitation is fixed at the nozzle throat; after that the cloud cavitation never disappears from the throat. On the other hand, the transition point of the N_2 test flowing through the orifice nozzle corresponds to point (d) in Figs. 3 – 5. As mentioned above, the cloud cavitation flowed from the nozzle throat outlet at point (d), i.e., the cloud cavitation developed within the throat before point (d), and it subsequently increased in the downstream section.

Table 2 Average reduction rate, R_d, of the pressure recovery ratio, R_p

Fluid	Throat	L_d/h_t or L_d/d_t	Re	R_d (s^{-1})	Step 1: R_d	Step 2: R_d
N_2	Orifice nozzle	38.0/2 = 19.0	0.221×10^6	0.297	a-d: 1.153	d-l: 0.145
N_2	C-D nozzle	45.6/2 = 22.8	0.202×10^6	0.303	a-k: 0.417	k-l: 0.261
He	C-D nozzle	43.8/2 = 21.9	4.12×10^6	1.103	a-e: 1.999	e-j: 0.821

L_d (mm): Axial length of the downstream zone of the throat in the video image, h_t (mm): Clearance of the orifice throat, d_t (mm): throat diameter of the C-D nozzle, Re: Reynolds number at the throat

The average reduction rate of R_p for each test series is presented in Table 2. It is found that the average reduction rate, R_d, of the helium R_p value is about three and a half times larger than that of N_2 in the transient growth process of the cloud cavitation. The transient growth process of the N_2 cloud cavitation can be divided into two steps, i.e., before and after the transition point. The value of R_d in step 1 before point (d) is almost eight times larger than that in step 2 after point (d) for the N_2 flowing through the orifice nozzle. In the test series of N_2 flowing through the C-D nozzle, the R_d value in step 1 before point (k) is over one and a half times larger than that in step 2 after point (k). However, each R_d value in the total growth process of the N_2 cloud cavitation is nearly the same value of 0.3 in spite of the difference in the throat configuration. However, a transition point corresponding to point (k) in the N_2 test was not identified in the He blowdown test because the He cloud cavitation was continuously produced near the upside of the nozzle throat and never disappeared from the visualization section after the initial nucleation. As described in the next section, reduction in the oscillation frequency of P_1 occurred suddenly at about point (e) in Fig. 9. Therefore, the transient growth process of the He cloud cavitation may be divided into two steps by selecting point (e) as the transition point. Table 2 shows that the helium R_d value in step 1 before point (e) is about two and a half times larger than that in step 2 after point (e). From the results, the basic characteristics of the transient growth process of the cloud cavitation observed in the blowdown test series are summarized in Fig.11.

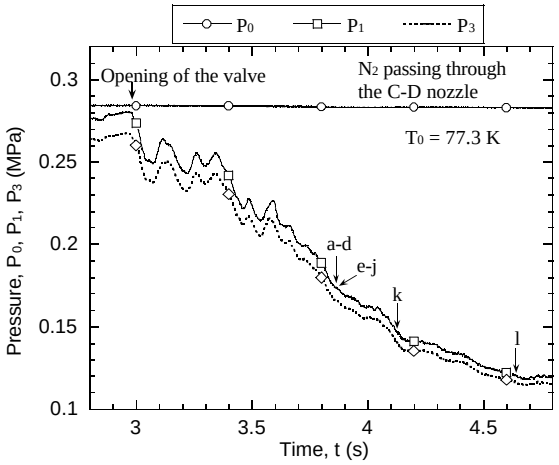

Fig. 6 Pressure measurements of N_2 flow, C-D nozzle

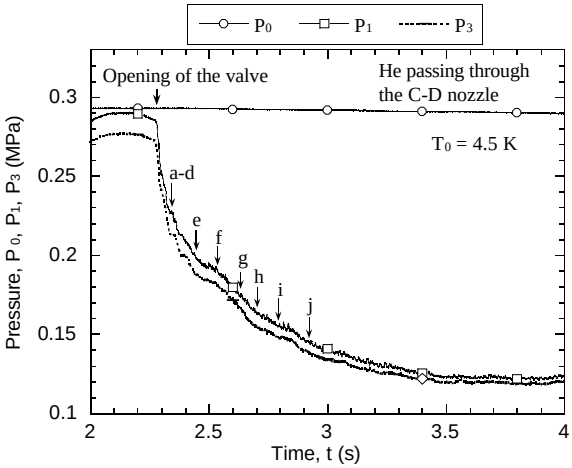

Fig. 8 Pressure measurements of He flow, C-D nozzle

Throat → Downstream

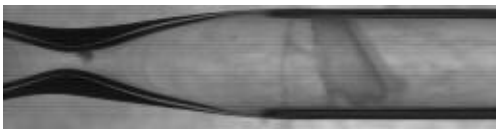

(a) t = 3.8482 s (0.8862 s ; from opening of the valve)

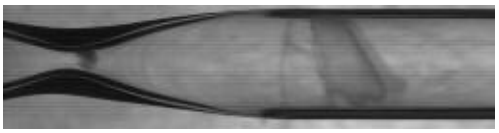

(b) t = 3.8483 (0.8862 s)

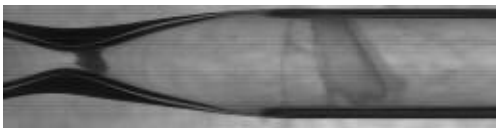

(c) t = 3.8484 s (0.8864 s)

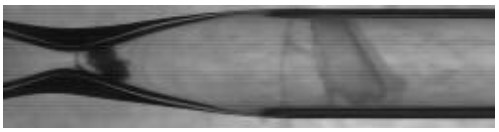

(d) t = 3.8487 s (0.8867 s)

Initial nucleation of cloud cavitaion at the throat

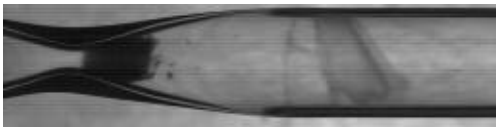

(e) t = 3.8577 s (0.8957 s)

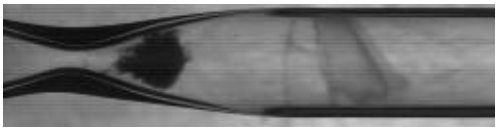

(f) t = 3.8583 s (0.8903 s)

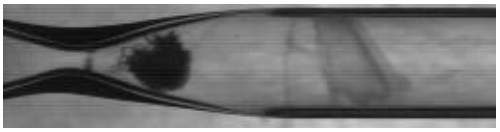

(g) t = 3.8584 s (0.8964 s)

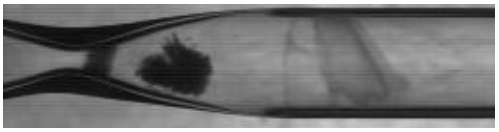

(h) t = 3.8587 s (0.8967 s)

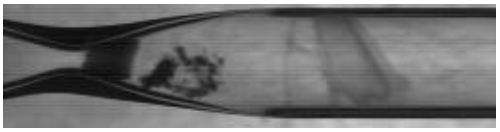

(i) t = 3.8589 s (0.8969 s)

(j) t = 3.8592 s (0.8792 s)

Nucleation-collapse cycle of cloud cavitation

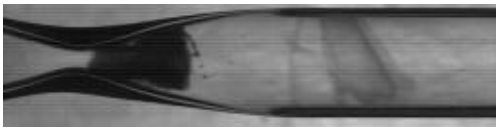

(k) t = 4.114 s (1.152 s)

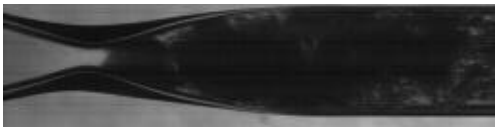

(l) t = 4.632 s (1.670 s)

Fig. 7 High-speed observations of N_2 flowing through the convergent-divergent nozzle

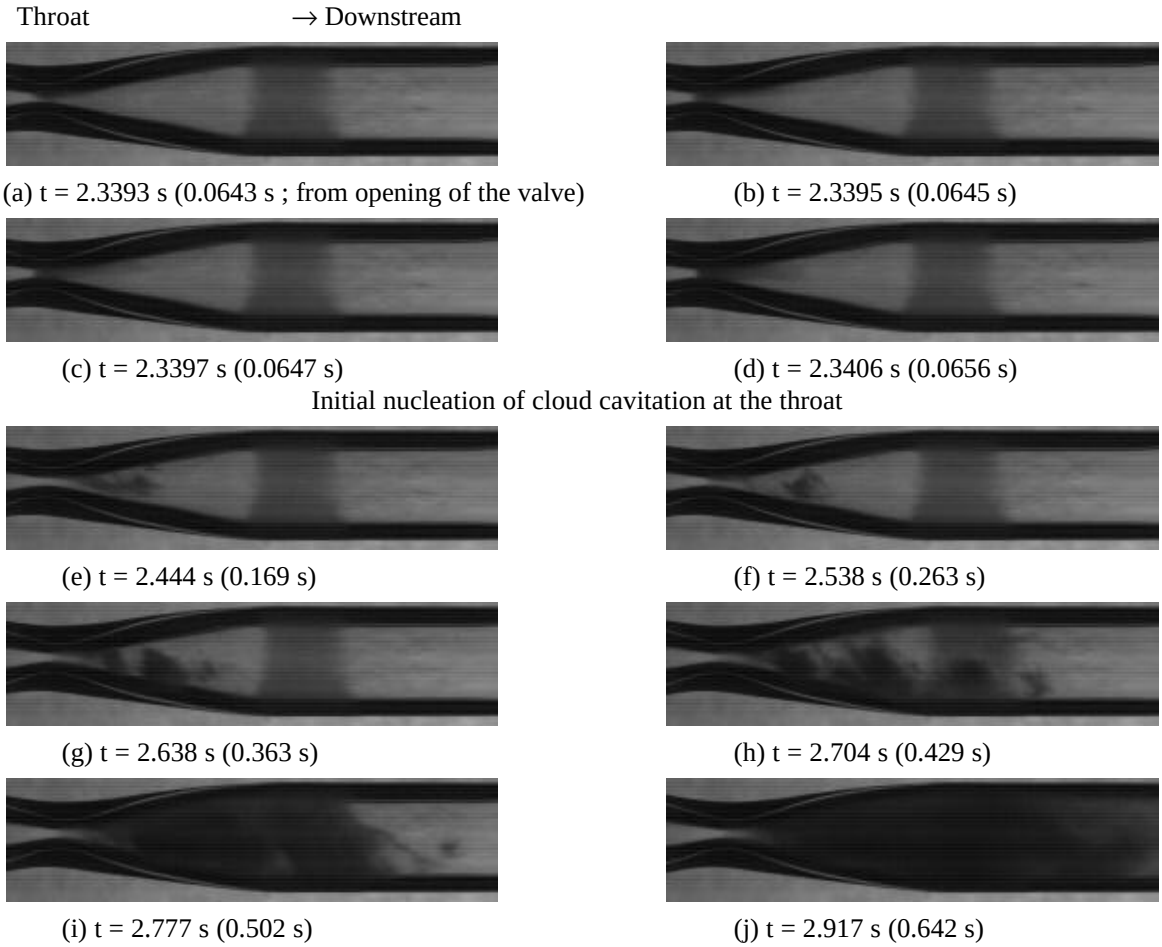

Fig. 9 High-speed observations of He flowing through the convergent-divergent nozzle

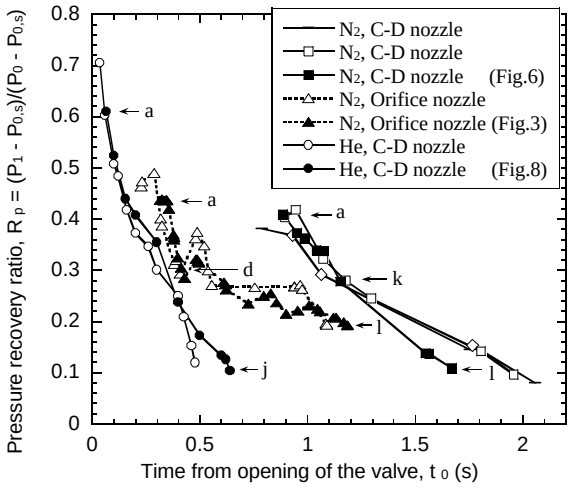

Fig. 10 Variation of pressure recovery ratio, R_p

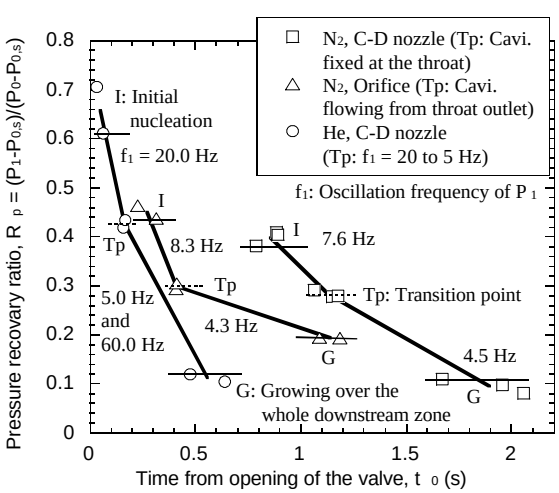

Fig. 11 Characteristics of the transient growth process

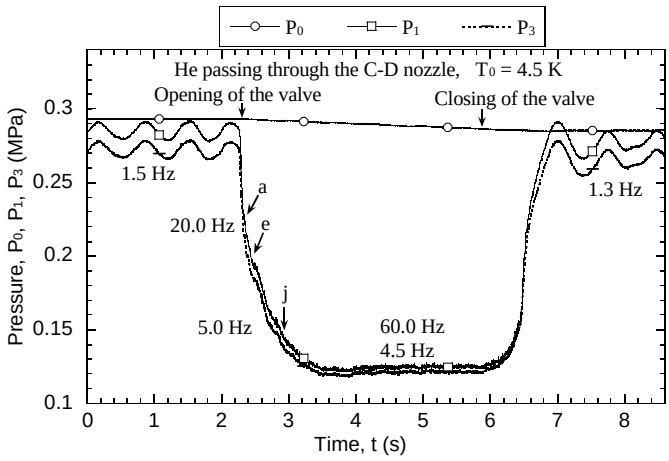

Fig. 12 Pressure oscillations of He flowing through the convergent-divergent nozzle

4 Flow instability

Figure 12 shows pressure oscillations obtained in the blowdown and shutoff test of He flowing through the C-D nozzle. Main oscillation frequencies, f_1, of P_1 at specific intervals are also presented in Figs. 12. In general, two types of instability are considered to occur in a cryogenic flow system. One is the instability induced by density wave oscillation and the other is that induced by acoustic wave oscillation. The density wave instability is characterized by a relatively low frequency because the period is of the same order as the resident time of a fluid particle in the line (Hands 1975). For the He blowdown tests, the maximum flow velocity of He in the throat downstream line is estimated to be about 17 m/s based on the pressure measurements around the orifice flowmeter installed in the downstream line. Therefore, the He instability with a frequency of less than 5.0 Hz is considered to be density wave oscillation. The pressure instability with a frequency of more than 20.0 Hz may be considered to be acoustic wave oscillation. From these results, it is found that the pressure instability in the He blowdown and shutoff test can be characterized as follows: density wave instability with a relatively large amplitude occurs before blowdown and after shutoff; pressure fluctuation of the transient flow is much smaller than that of N_2; pressure instability with high-frequency and small amplitude occurs under the condition of steady blowdown.

5 Conclusions

A flow visualization study on two-phase cryogenic flows passing through a convergent-divergent nozzle or an orifice nozzle installed in a horizontal pipe was carried out to clarify the fundamental characteristics of the transient growth process of He cloud cavitation based on a comparison between liquid He and liquid N_2. The basic characteristics of the transient growth process observed in the blowdown test series are summarized in Fig.11. They indicate that the transient growth process can be divided into two different steps by taking into account the transition point based on the observational results. Therefore, it was found that taking the transition phenomenon into account is one of the most effective ways to clarify the characteristics of the transient growth process. Based on the instable pressure oscillations observed in the blowdown and shutoff tests, it was found that the pressure instability of He is characterized as follows: (a) density wave instability with a relatively large amplitude occurs before blowdown and after shutoff; (b) pressure fluctuation of the transient flow is much smaller than that of N_2; (c) acoustic wave instability with high-frequency and small amplitude occurs under the steady blowdown condition.

References

Cheremisinoff, N. P. (1989). Encyclopedia of Fluid Mechanics Volume 8, Gulf Publishing Corp., Houston, Texas.
Filina, N. N. and Weisend, J. G. (1996). Cryogenic Two-Phase Flow, Camb. Univ. Press.
Filippov, Yu. P. (1999). Cryogenics, **39**, 59-75.
Hands, B. A. (1975). Adv. Cryogenic Engineering, **20**, 355-369.
Huang, X. and Van Sciver, S. W. (1994). Adv. Cryogenic Engineering, **39**, 1065-1071.
Kamijo, K., Yoshida, M. and Tujimoto, Y. (1993). J. Propulsion and Power, **9**, No. 6, 819-826.
King, J. A. (1972). NASA CR-123555.
Sauvage-Boutar, E., Meuris, C., Poivilliers, J. and Francois, M. X. (1987). Adv. Cryogenic Engineering, **32**, 441-447.